Efficient Fermionic One–Loop RG for the 2D Hubbard Model at Van Hove Filling

C. Husemann* and M. Salmhofer†

Institut für theoretische Physik, Universität Heidelberg

(Dated: February 10, 2009)

We propose a novel parametrization of the four–point vertex function in the one–loop one–particle irreducible renormalization group (RG) scheme for fermions. It is based on a decomposition of the effective two–fermion interaction into fermion bilinears that interact via exchange bosons. Besides being more efficient than previous N–patch schemes, this parametrization also reduces the ambiguity of introducing boson fields. We apply this parametrization to the two–dimensional (t, t')–Hubbard model using a novel Ω–frequency regularization.

Introduction. In the past decade the one–loop Wilsonian renormalization group (RG) has been extensively used to study the weak coupling instabilities of the two–dimensional (t, t')–Hubbard model [1, 2, 3, 4, 5, 6, 7, 8, 9, 10, 11, 12, 13]. Successes include the explanation of d–wave pairing tendencies from a repulsive interaction. The interplay of antiferromagnetic and d–wave superconducting instabilities found for small next to nearest neighbor hopping $-t'$ resembles the behavior of the high temperature cuprates near half filling. Avoiding the artificial suppression of small momentum particle–hole fluctuations by regularizing with temperature, the leading instability for strong hopping $-t'$ was found to be ferromagnetism at Van Hove filling and triplet superconductivity away from Van Hove filling [9, 14].

The one–loop truncation in the one–particle irreducible RG scheme results in an integro–differential equation for the four–point vertex function and the self–energy [15]. The studies mentioned in the last paragraph neglect the self–energy and the frequency dependence of the four–point function. The remaining three independent momenta of the four–point function (one is determined by momentum conservation) are numerically discretized with N patches in momentum space. In most studies these have been chosen along the Fermi surface by power counting arguments. Then a system of ordinary differential equations of size $\sim N^3$ has to be solved numerically. Generically for the two–dimensional Hubbard model at low temperature, some coupling constants, which describe the vertex function for certain momentum combinations, grow large. In order to determine the nature of the corresponding instability, susceptibilities are calculated in the flow by introducing external boson fields coupled to appropriate fermion bilinears [15].

In this work we develop a novel parametrization of the four–point function in the one–particle irreducible RG scheme. Guided by the singular momentum structure of the right hand side of the flow equation, we identify three channels with distinct singular momentum structures. In these channels the effective two–fermion interaction is expanded in fermion bilinears that interact via exchange bosons. These bosons, however, are dealt with in a purely fermionic language. We show that only a small number of terms is needed to capture the essential features of the one–loop RG flow. This improves the efficiency of the parametrization compared to previous N–patch schemes. A similar reduction has recently been used for the single impurity Anderson model [16]. We apply the method to the two–dimensional Hubbard model at Van Hove filling and compare the results with the temperature RG flow [9]. Instead of regularizing with temperature, we introduce a novel frequency regularization scheme with scale parameter Ω.

Decomposition of the Effective Interaction. Although the initial vertex function of the Hubbard model at high scales is a constant in momentum space, according to the RG equation a non–trivial momentum structure evolves in the flow as the scale is lowered. The instabilities of the RG flow, are however mainly determined by the singular momentum structure of the right hand side of the RG equation. Therefore, we develop a parametrization of the vertex function that simplifies the momentum dependence but keeps track of all possible singular contributions. As long as the vertex function is still regular, the only momentum dependence that can change the singular behavior of the RG equation is the transfer momentum that flows through the scale–derivative of the particle–particle or particle–hole two–fermion bubble.

On the right hand side of the RG equation three different classes of graphs with distinct transfer momenta contribute – the particle–particle graph, the crossed particle–hole graph, and the direct particle–hole graphs [15]. Accordingly, we identify three different channels, which we first assume as general charge and spin rotation invariant two–fermion interactions. They are defined by three conditions: (1) each vertex function of the channels absorbs one singular momentum, that is, one transfer momentum; (2) the channels describe the interaction of Cooper pairs, spin operators, and density operators, respectively, if the transfer momentum becomes singular; and (3) each channel separately satisfies particle–hole symmetry and the fermionic antisymmetry. Then the evolution of the superconducting channel is given by the particle–particle graph, of the magnetic channel by the crossed particle–hole graph, and of the forward scattering channel by a combination of crossed and direct particle–hole graphs, see Figure 1. The vertices in Figure 1 depict the fermionic irreducible four–point vertex

$V_\Omega(k_1, k_2, k_3)$, where we denote momentum $\mathbf{k}$ and frequency k_0 together by $k = (\mathbf{k}, k_0)$. Spin is conserved along the fermion lines, see [15].

$$\dot{\Phi}^\Omega_{\text{SC}}(k_1, k_3, k_1 + k_2) \;=\; -$$

$$\dot{\Phi}^\Omega_{\text{M}}(k_1, k_2, k_3 - k_1) \;=\;$$

$$\dot{\Phi}^\Omega_{\text{K}}(k_1, k_2, k_2 - k_3) \;=\; 4 \qquad -2$$
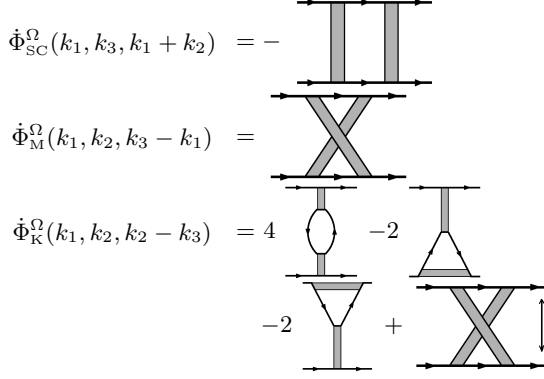
$$-2 \qquad +$$

FIG. 1: Evolution of the superconducting, magnetic, and forward scattering channel respectively. The dot stands for a derivative with respect to the scale Ω and the doublesided arrow in the last graph symbols the exchange of two momenta and frequencies.

The initial condition for the channels is zero, so they are generated in the flow. The full vertex function of the Hubbard model is then given by the sum

$$V_\Omega(k_1, k_2, k_3) = U - \Phi^\Omega_{\text{SC}}(k_1, k_3, k_1 + k_2)$$
$$+ \Phi^\Omega_{\text{M}}(k_1, k_2, k_3 - k_1) + \frac{1}{2}\Phi^\Omega_{\text{M}}(k_1, k_2, k_2 - k_3) \qquad (1)$$
$$- \frac{1}{2}\Phi^\Omega_{\text{K}}(k_1, k_2, k_2 - k_3)\,.$$

This decomposition is exact on one–loop level since all graphs with their full momentum and frequency dependence are taken into account. The assignment of the graphs, however, can be ambiguous for special momenta. Using the Fierz identity, for example, a constant term can be freely distributed among the channels. This is why the initial Hubbard repulsion U is not decomposed and kept explicitly in the decomposition as a constant. However, this does not mean that the on–site term in the full interaction remains independent of scale. The corrections to it are rather absorbed as contributions to the above defined three channels.

Next we further decompose the two–fermion interaction by writing each channel as a sum of terms, in which two fermion bilinears interact via an exchange boson propagator, where the boson momentum is the corresponding singular transfer momentum of the channel. For fixed transfer momentum l the vertex function $\Phi^\Omega_{\text{SC}}(q, q', l) = \Phi^\Omega_{\text{SC}}(q', q, l)$ can be seen as the kernel of a Fredholm operator. Therefore, due to compactness, a diagonal expansion in eigenfunctions is possible in principle. To avoid a calculation of the (scale–dependent) eigenfunctions, we simply expand in an orthonormal basis of $L^2((-\pi, \pi]^2)$ of form factors f_n that represent the

point symmetry group of the lattice. Then, the expansion involves non–diagonal terms

$$\Phi^\Omega_{\text{SC}}(q, q', l) = \sum_{m,n \in \mathcal{I}} D^\Omega_{mn}(l) f_m(\tfrac{1}{2} - \mathbf{q}) f_n(\tfrac{1}{2} - \mathbf{q}')$$
$$+ R^\Omega_{\text{SC}}(q, q', l)\,. \qquad (2)$$

For simplicity the form functions are chosen frequency independent here. The expansion coefficients $D^\Omega_{mn}(l)$ depend on the transfer momentum and frequency l and are called superconducting boson propagators. In practise, we restrict to a finite set $\mathcal{I}$ of terms. The remainder function R^Ω_{SC} accounts for the error.

Similarly, the magnetic and forward scattering channels are expanded in appropriate frequency and scale independent form factors

$$\Phi^\Omega_{\text{M}}(q, q', l) = \sum_{m,n \in \mathcal{I}} M^\Omega_{mn}(l) f_m(\mathbf{q} + \tfrac{1}{2}) f_n(\mathbf{q}' - \tfrac{1}{2})$$
$$+ R^\Omega_{\text{M}}(q, q', l) \qquad (3)$$
$$\Phi^\Omega_{\text{K}}(q, q', l) = \sum_{m,n \in \mathcal{I}} K^\Omega_{mn}(l) f_m(\mathbf{q} + \tfrac{1}{2}) f_n(\mathbf{q}' - \tfrac{1}{2})$$
$$+ R^\Omega_{\text{K}}(q, q', l)\,. \qquad (4)$$

This introduces the magnetic boson propagators M^Ω_{mn}, the forward scattering boson propagators K^Ω_{mn}, and additonal remainder terms.

The Flow of Boson Propagators. The flow equations for the boson propagators are obtained by inserting the proposed decomposition in the RG equation for the vertex function [15] and projecting each channel onto the coefficients of the orthogonal form factor expansion. If the remainder terms are dropped, this gives a closed system of integro–differential equations for the boson propagators. Compared to the original RG equation for the vertex function, their solution is now given by several functions dependent on one momentum and frequency instead of one function dependent on three momenta and frequencies. This is a considerable simplification and, in particular, makes the numerical implementation more favorable. Furthermore, like the two–fermion bubbles, the boson propagators have only point singularities in momentum space instead of extended Fermi surface singularities.

In the case of a regular Fermi surface with irrelevant Umklapp scattering the RG flow is dominated by the superconducting boson propagators if the initial interaction contains an attractive part. This scenario is well understood even analytically and there are clear arguments which form factors have to be chosen, such that the remainder terms are negligible. If the initial interaction is purely repulsive, we are able to show that contributions of the magnetic channel induce an attractive d–wave pairing interaction in the superconducting channel.

At Van Hove filling, however, the Fermi surface has saddle points, which cause a logarithmic singularity in

the density of states. Furthermore, near half filling, Umklapp scattering processes become relevant. Then there is strong mixing between particle–particle and particle–hole channels. This case is not analytically understood yet and treated numerically in the following. Here the form factors are chosen guided by previous N–patch studies and the remainder terms are neglected. A rigorous analysis of the remainder terms is left for future work.

The numerical implementation of the boson propagator flow is eased by specifying the momentum and frequency dependence of the boson propagators. Here we first neglect the frequency dependence of the boson propagators. Together with the frequency independent form factors, this corresponds to a vertex function that does not depend on frequency at all. The right hand side of the flow equations is evaluated at boson frequency zero, which gives the main contribution. An analysis of the two–fermion bubbles indicates that the boson propagators can only become singular at boson momentum $(0,0)$ and (π,π). Therefore we split up each boson propagator into a part around $(0,0)$ and a part around (π,π). In these regions we parameterize the momentum dependence of the boson propagators by step functions, postulating a higher accuracy at the singular points. For example, a peak of the magnetic boson propagator $M_{\mathrm{SS}}(\mathbf{l})$ with constant form factor $f_{\mathrm{s}}(\mathbf{q}) = 1$ at $\mathbf{l} = (0,0)$ indicates ferromagnetic and at $\mathbf{l} = (\pi,\pi)$ antiferromagnetic fluctuations.

In order to set up the RG flow, a regularization parameterized by an RG scale has to be introduced. Since we are especially interested in the interplay between d–wave superconductivity and ferromagnetism, we have to choose a regularization that is sensitive to small momentum particle–hole fluctuations [9]. Here we introduce a frequency regularization by multiplying the bare propagator with the function

$$\chi_\Omega(p) = \frac{p_0^2}{p_0^2 + \Omega^2} \ , \tag{5}$$

where p_0 is the frequency part of p and Ω is the RG scale frequency. For $\Omega > 0$ all graphs are regularized in the infrared and for $\Omega \to 0$ the original model is recovered. Unlike a Fermi surface cut–off, this regularization reproduces the correct $(\ln \Omega)^2$–scaling of the particle–particle and $\ln \Omega$–scaling for the particle–hole bubble at Van Hove filling. Compared to the temperature flow, this regularization allows a clear definition of the initial condition of the RG flow. We start the flow at a high initial scale Ω_0 and treat the scales $\Omega > \Omega_0$ by perturbation theory in the coupling constant $U > 0$ to second order. Due to the infrared regularization, perturbation theory converges if U/Ω_0 is small enough. For large enough Ω_0, we find that the dependence on Ω_0 is negligible.

Results and Outlook. Here we present results obtained by expanding each channel with two form factors, namely isotropic s–wave $f_{\mathrm{s}}(\mathbf{q}) = 1$ and $d_{x^2-y^2}$–
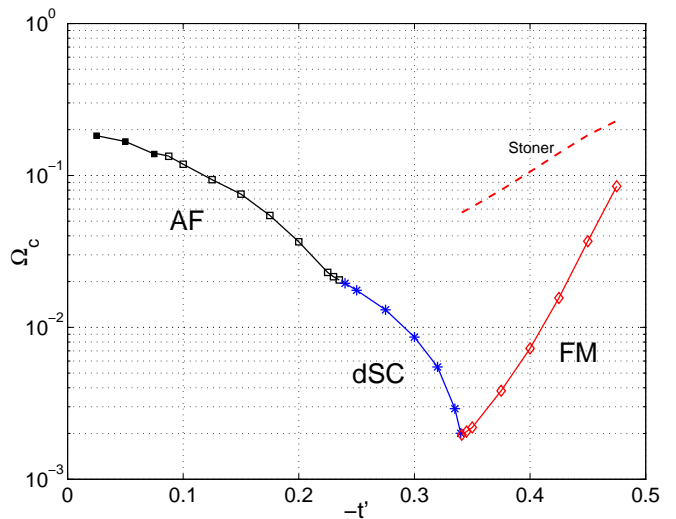

FIG. 2: The critical scale Ω_{C} in dependence on next to nearest neighbor hopping $-t'$ at temperature zero with initial scale $\Omega_0 = 15t$. The chemical potential is set to match Van Hove filling at each $-t'$. The instabilities of the Landau Fermi liquid are determined as antiferromagnetism (AF), $d_{x^2-y^2}$–superconductivity (dSC), and ferromagnetism (FM).

wave $f_1(\mathbf{q}) = \cos q_1 - \cos q_2$. Amongst others, the corresponding boson propagators allow to detect instabilities towards s– and $d_{x^2-y^2}$–wave superconductivity, ferro– and antiferromagnetism, forward and exchange scattering, and also a Pomeranchuk instability. It turned out, however, that the boson propagator flow applied to the (t,t')–Hubbard model at zero temperature and Van Hove filling already gives reasonable results if only the constant form factor is taken into account in every channel plus the $d_{x^2-y^2}$–wave form factor in the superconducting channel. Although s–wave superconductivity is suppressed by the initial repulsion, its screening effect is essential for the RG flow.

Starting from $U = 3t$ we observe a generic flow to strong coupling. If the maximum of one boson propagator reaches the value $20t$, the flow is manually stopped at the thus defined "critical" scale Ω_{C}. Like in the previous N–patch studies of the symmetric phase, this is interpreted as an instability towards a corresponding ordered state. The critical scale Ω_{C} is plotted over next to nearest neighbor hopping $-t'/t$ in Figure 2, where from now on $t = 1$. For small $-t'$, where Van Hove filling is close to half filling, antiferromagnetism dominates. Since the flow is stopped at a relatively high scale, perfect nesting–like effects are not restricted to $-t' = 0$. If $-t'$ is increased, we observe a tendency to incommensurate antiferromagnetic order (marked with open squares). For intermediate $-t'$ the leading instability is $d_{x^2-y^2}$–superconductivity. It is induced by antiferromagnetic fluctuations, as can be seen from the flow equations. For high $-t'$ ferromagnetism is the dominant instability. In the interval

$-t' \in (0, 0.34)$ the critical scale drops by two orders of magnitude.

The results obtained with the decomposed RG flow agree well with the temperature N–patch flow [9]. The proposed approximation to the one–loop RG flow reproduces the qualitative instabilities and the values for $-t'$, where the transitions between different instabilities take place. Indicated by the decreased critical scale, $d_{x^2-y^2}$–superconductivity and ferromagnetism suppress each other. For comparison, the Stoner criterion for ferromagnetism, which is obtained by neglecting the particle–particle channel, is plotted in Figure 2 on the ferromagnetic side. There is one significant deviation from the temperature flow: in our present scheme, the suppression of Ω_C in the transition region from d–wave superconductivity to ferromagnetism is much weaker. Since both the temperature flow and our calculation involve approxiamtions, the existence of a quantum critical point remains an open question.

In summary, the proposed decomposition of the effective two–fermion interaction is efficient for studying competing instabilities in the (t, t')–Hubbard model. Separating leading from subleading processes reduces the complexity of the one–loop flow equations. Although we cannot yet rigorously justify dropping the remainder terms at Van Hove filling, there are clear arguments for this for regular Fermi surfaces. In fact, the comparison with previous N–patch studies shows that the qualitative structure of the RG flow is preserved.

In the numerical implementation the momentum dependence of the boson propagators is discretized using step functions. This is more precise than the general patching in N–patch schemes since the choice of step functions can be guided by the one–loop bubbles. Generally, if the momentum dependence of the one–loop bubbles can be is parameterized in an analytical form, then it is possible to extract a functional parametrization of the boson propagators from the flow equations, at least for small momenta. Similarly, the dependence on small frequencies can be taken into account. Deviations from the large frequency behavior would then be subject to further remainder terms.

The decomposition of the effective two–fermion interaction into sums of fermion bilinears interacting via boson propagators allows to decouple the fermion bilinears by multiple Hubbard Stratonovich transformations. Thereby the ambiguity of introducing boson fields is not completely removed as discussed above. However, due to the definition of the channels based on the singular momentum structure, it is reduced. Thus our results serve as an improved starting point for a continuation of the RG flow into the symmetry broken phase in a (partially) bosonized form [17, 18, 19, 20, 21].

————————

[*] Electronic address: c.husemann@thphys.uni-heidelberg.de

[†] Electronic address: m.salmhofer@thphys.uni-heidelberg.de

[1] D. Zanchi and H. J. Schulz, Europhys. Lett. **44**, 235 (1998).

[2] D. Zanchi and H. J. Schulz, Phys. Rev. B **61**, 13609 (2000).

[3] C. J. Halboth and W. Metzner, Phys. Rev. B **61**, 7364 (2000).

[4] C. J. Halboth and W. Metzner, Phys. Rev. Lett. **85**, 5162 (2000).

[5] D. Zanchi, Europhys. Lett. **55**, 376 (2001).

[6] C. Honerkamp, M. Salmhofer, N. Furukawa, and T. M. Rice, Phys. Rev. B **63**, 035109 (2001).

[7] D. Rohe and W. Metzner, Phys. Rev. B **71**, 115116 (2005).

[8] C. Honerkamp and M. Salmhofer, Phys. Rev. B **67**, 174504 (2003).

[9] C. Honerkamp and M. Salmhofer, Phys. Rev. B **64**, 184516 (2001).

[10] A. A. Katanin and A. P. Kampf, Phys. Rev. B **68**, 195101 (2003).

[11] A. A. Katanin and A. P. Kampf, Phys. Rev. Lett. **93**, 106406 (2004).

[12] C. Honerkamp, D. Rohe, S. Andergassen, and T. Enss, Phys. Rev. B **70**, 235115 (2004).

[13] C. Honerkamp, Eur. Phys. J. B **21**, 81 (2001).

[14] C. Honerkamp and M. Salmhofer, Phys. Rev. Lett. **87**, 187004 (2001).

[15] M. Salmhofer and C. Honerkamp, Prog. Theor. Phys. **105**, 1 (2001).

[16] C. Karrasch, R. Hedden, R. Peters, T. Pruschke, K. Schönhammer, and V. Meden, J. Phys.: Cond. Matt. **20**, 345205 (2008).

[17] P. Strack, R. Gersch, and W. Metzner (2008), arXiv:0804.3994v1.

[18] H. C. Krahl, J. A. Müller, and C. Wetterich (2008), arXiv:0801.1773v1.

[19] T. Baier, E. Bick, and C. Wetterich, Phys. Rev. B **70**, 125111 (2004).

[20] F. Schütz, L. Bartosch, and P. Kopietz, Phys. Rev. B **72**, 035107 (2005).

[21] J. Reiss, D. Rohe, and W. Metzner, Phys. Rev. B **75**, 075110 (2007).